

Bayesian Variable Selection for High-Dimensional Mediation Analysis: Application to Metabolomics Data in Epidemiological Studies

Youngho Bae¹, Chanmin Kim¹, Fenglei Wang², Qi Sun^{2,3,4}, Kyu Ha Lee^{2,3,5,*}

¹*Department of Statistics, Sungkyunkwan University, Seoul, South Korea*

²*Department of Nutrition, Harvard T.H. Chan School of Public Health, Boston, MA, U.S.A.*

³*Department of Epidemiology, Harvard T.H. Chan School of Public Health, Boston, MA, U.S.A.*

⁴*Channing Division of Network Medicine, Brigham and Women's Hospital, Boston, MA, U.S.A.*

⁵*Department of Biostatistics, Harvard T.H. Chan School of Public Health, Boston, MA, U.S.A.*

*klee@hsph.harvard.edu

Abstract

In epidemiological research, causal models incorporating potential mediators along a pathway are crucial for understanding how exposures influence health outcomes. This work is motivated by integrated epidemiological and blood biomarker studies, investigating the relationship between long-term adherence to a Mediterranean diet and cardiometabolic health, with plasma metabolomes as potential mediators. Analyzing causal mediation in such high-dimensional omics data presents substantial challenges, including complex dependencies among mediators and the need for advanced regularization or Bayesian techniques to ensure stable and interpretable estimation and selection of indirect effects. To this end, we propose a novel Bayesian framework for identifying active pathways and estimating indirect effects in the presence of high-dimensional multivariate mediators. Our approach adopts a multivariate stochastic search variable selection method, tailored for such complex mediation scenarios. Central to our method is the introduction of a set of priors for the selection indicators in the mediator and outcome models: a Markov random field prior and sequential subsetting Bernoulli priors. The first prior's Markov property leverages the inherent correlations among mediators, thereby increasing power to detect mediated effects.

The sequential subsetting aspect of the second prior encourages the simultaneous selection of relevant mediators and their corresponding indirect effects from the two model parts, providing a more coherent and efficient variable selection framework, specific to mediation analysis. Comprehensive simulation studies demonstrate that the proposed method provides superior power in detecting active mediating pathways. We further illustrate the practical utility of the method through its application to metabolome data from two sub-studies within the Health Professionals Follow-up Study and Nurses' Health Study II, highlighting its effectiveness in real data setting.

Keywords: Bayesian variable selection, indirect effects, mediation analysis, metabolomics data, phase transition, spike-and-slab prior

1 Introduction

Mediation analysis is a powerful tool in epidemiological research, allowing for a deeper understanding of the biological mechanisms through which exposures influence health outcomes. In studies that integrate blood biomarkers, the use of high-dimensional omics measures as mediators offers a unique opportunity to identify the pathways between exposures and health conditions. For instance, in our motivating epidemiological studies exploring the association between long-term adherence to a Mediterranean diet and cardiometabolic health, metabolomic profiles can serve as key mediators by capturing the small-molecule metabolites that reflect biochemical processes triggered by diet.

This work is motivated by two substudies within the Health Professionals Follow-up Study (HPFS) and Nurses' Health Study II (NHSII). The HPFS and the NHSII are ongoing prospective cohort studies involving 51,529 U.S. male health professionals, initiated in 1986 (Rimm et al., 1991), and 116,429 female registered nurses, initiated in 1989 (Bao et al., 2016), respectively. Detailed participant information on diet, lifestyle, medication use, and health outcomes was collected at baseline and updated biennially. The substudies include 307 men and 233 women, all free from coronary heart disease, stroke, cancer, or major

neurological diseases, and involve the collection of blood samples from participants (Huang et al., 2019; Wang et al., 2021). Metabolomics data derived from blood biomarkers have been extensively analyzed in impactful studies, including investigations into the association between plasma metabolite profiles linked to plant-based diets and type 2 diabetes (Wang et al., 2022), and the pivotal role of these profiles in mediating the relationship between haem iron intake and type 2 diabetes risk (Wang et al., 2024). Our analysis in this work focuses on (i) identifying a subset of metabolites that mediate the relationship between adherence to a Mediterranean diet and cardiometabolic health outcomes, and (ii) estimating and making inferences about the indirect effect sizes associated with these metabolites.

Broadly, published methodologies for mediation analysis with high-dimensional mediators can be categorized into three main approaches: methods employing dimension reduction techniques, such as principal component analysis and its variants (Huang and Pan, 2016; Chén et al., 2018; Zhao et al., 2020), as well as latent mediator models (Derkach et al., 2019); penalization-based methods that apply regularization techniques to reduce the set of potential mediators before mediator-outcome analysis (Zhang et al., 2016; Gao et al., 2019; Perera et al., 2022; Zhang, 2022; Zhao and Luo, 2022); and joint modeling frameworks, which estimate exposure-mediator-outcome pathways simultaneously, addressing uncertainties across all stages of estimation (Aung et al., 2020; Song et al., 2020, 2021a,b). Each strategy has certain limitations. For instance, dimension reduction techniques condense information from multiple mediators but restrict the ability to interpret mediation effects at the individual mediator level. Similarly, penalization-based methods, which follow a two-stage approach, do not adequately account for uncertainty estimated from the selection of mediators, potentially biasing downstream mediator-outcome inference. In contrast, joint modeling frameworks overcome these limitations by unifying pathway estimation; however, the existing methods assume independent mediators or employ simple latent

neighboring structures with limited connectivity between mediators (Song et al., 2021a), likely due to the challenges of computational complexity. Moreover, a common drawback across these approaches is their tendency to overlook correlations among mediators (Figure 1). As demonstrated in the multivariate analysis literature (Breiman and Friedman, 1997; Saccenti et al., 2014; Lee et al., 2017, 2020), ignoring these dependencies can lead to inflated false positive rates, reduced statistical power, and decreased predictability. To our knowledge, no existing statistical methods for joint mediation analysis leverage mediator correlations through specialized priors or penalty terms to enhance the detection of active mediating pathways.

Toward overcoming these limitations, we propose a novel Bayesian mediation analysis method that identifies active exposure–mediator–outcome pathways and estimates the corresponding indirect effects within a joint modeling framework, while accommodating correlations among high-dimensional mediators. The foundation of our approach lies in the introduction of a Markov random field (MRF) and a conditional Bernoulli prior for latent binary selection indicators in the mediator and outcome models, respectively. The application of these priors in mediation analysis offers advantages in two key aspects. First, it leverages the covariance structure among mediators by specifying edge potentials within the MRFs. This structure is adaptively updated at each step of the Markov chain Monte Carlo (MCMC) algorithm, enabling variable selection to account for both the mean model and variance-covariance structure of the mediators. Second, the sequential subsetting nature of the conditional Bernoulli prior promotes simultaneous selection of relevant mediators and their indirect effects across both mediator and outcome models, leading to a more coherent and efficient variable selection procedure for mediation analysis.

The remainder of this article is organized as follows: Section 2 outlines the high-dimensional mediation analysis framework, including observed data model and identifying

assumptions; Section 3 details the proposed Bayesian framework, including the specification of prior distributions and an overview of an efficient computational algorithm for sampling from the joint posterior distribution; Section 4 presents comprehensive simulation studies assessing the performance of the proposed framework; Section 5 provides an detailed analysis of the motivating NHSII/HPFS substudies; and Section 6 concludes the article with a discussion. Supplementary details, including computational algorithms and additional results, are provided in an online materials document as appropriate.

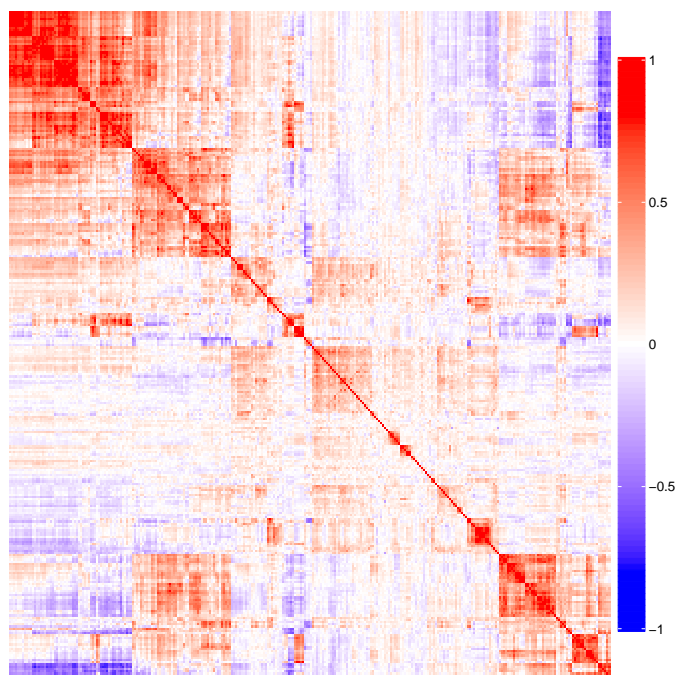


Figure 1: Empirical correlations among the measures of 298 metabolites in the substudies within the Health Professionals Follow-up Study (HPFS) and Nurses' Health Study II (NHSII).

2 High-dimensional Mediation Analysis

Let A_i represent an exposure for $i = 1, \dots, n$. Within the potential outcomes framework (Rubin, 1974), define $\mathbf{M}_i(a) = \{M_{1,i}(a), M_{2,i}(a), \dots, M_{q,i}(a)\}$ as the potential values of the q -dimensional mediators for the i -th observation under exposure level $A_i = a$. Additionally, let $Y_i(a, \mathbf{m})$ represent the potential outcome that would be observed under exposure status a and mediator vector \mathbf{m} . Assuming the commonly applied Stable Unit Treatment Value Assumption (SUTVA) (Rubin, 1990; Forastiere et al., 2016), each potential mediator and outcome can be linked to the observed data as follows: $M_{j,i}(A_i) = M_{j,i}$ for $j = 1, \dots, q$ and $Y_i(A_i, \mathbf{M}_i) = Y_i$. This implies that the potential mediators and outcome at the actual treatment level A_i received by the i -th unit are equivalent to the observed values.

In the presence of high-dimensional mediators, we assume that each mediator operates through an independent pathway between the exposure and the outcome. As illustrated in Figure 2, we adopt a sparsity assumption, where only a subset of the high-dimensional mediators have active pathways for both exposure-mediator and mediator-outcome relationships. Additionally, we allow for correlated (non-causal) relationships among the mediators.

In this setting, the target causal estimand is the active mediation effect, defined as the average effect from the mediation pathways where both pathways centered around each mediator are active. Formally, if the j -th mediator has an active pathway, the indirect effect for two different exposure levels a and a' ($IE_j(a, a')$) through this pathway is defined as follows:

$$IE_j(a, a') = E[Y_i(a, \{M_{1,i}(a), M_{2,i}(a), \dots, M_{q,i}(a)\}) - Y_i(a, \{M_{1,i}(a), M_{2,i}(a), \dots, M_{j-1,i}(a), M_{j,i}(a'), M_{j+1,i}(a), \dots, M_{q,i}(a)\})].$$

Furthermore, the sum of all indirect effects ($IE(a, a')$) through the active mediators and

the direct effect ($DE(a, a')$) not mediated through any mediator are as follows:

$$IE(a, a') = \sum_{j \in \mathcal{M}} IE_j(a, a'),$$

$$DE(a, a') = E[Y_i(a, \{M_{1,i}(a'), M_{2,i}(a'), \dots, M_{q,i}(a')\}) - Y_i(a', \{M_{1,i}(a'), M_{2,i}(a'), \dots, M_{q,i}(a')\})],$$

where \mathcal{M} denotes the set of indices for mediators with active mediation pathways.

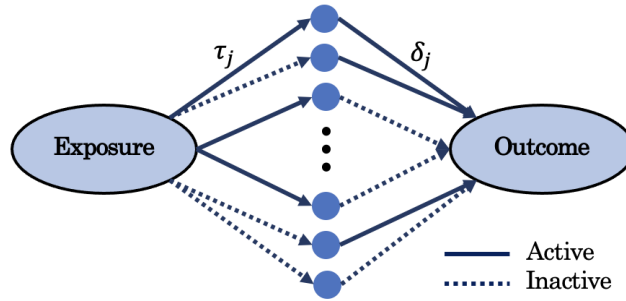


Figure 2: A directed acyclic graph illustrating high-dimensional mediators. Each mediator has an independent pathway, with the treatment-mediator and mediator-outcome pathways able to independently activate or deactivate. A causal effect is transmitted through a mediator only when both pathways are active. A correlation structure among mediators is also permitted.

2.1 Observed data model

Let \mathbf{X}_i , A_i , \mathbf{M}_i , and Y_i represent the p -dimensional vector of covariates, exposure, q -dimensional mediators, and the outcome for the i -th subject, respectively. The observed

data models for the high-dimensional mediators and the outcome are specified as follows:

$$\mathbf{M}_i = \boldsymbol{\beta}_0 + \boldsymbol{\tau}A_i + B^\top \mathbf{X}_i + \epsilon_M, \quad \epsilon_M \sim \text{MVN}(\mathbf{0}, \Sigma), \quad (1)$$

$$Y_i = \alpha_0 + \boldsymbol{\delta}^\top \mathbf{M}_i + \boldsymbol{\alpha}^\top \mathbf{X}_i + \alpha_{p+1}A_i + \epsilon_Y, \quad \epsilon_Y \sim \text{Normal}(0, \sigma^2), \quad (2)$$

where $\boldsymbol{\beta}_0 = (\beta_{0,1}, \dots, \beta_{0,q})^\top$ denotes the intercepts, and B is the $p \times q$ matrix with columns $\boldsymbol{\beta}_1, \dots, \boldsymbol{\beta}_q$, where $\boldsymbol{\beta}_j = (\beta_{j,1}, \dots, \beta_{j,p})^\top$ for $j = 1, \dots, q$. The vector $\boldsymbol{\tau} = (\tau_1, \dots, \tau_q)^\top$ captures the effects of exposure A_i on the corresponding mediators, and Σ is the variance-covariance matrix of a multivariate normal (MVN), allowing for associational relationships among the mediators. In the outcome model, $\boldsymbol{\delta} = (\delta_1, \dots, \delta_q)^\top$ and $\boldsymbol{\alpha} = (\alpha_1, \alpha_2, \dots, \alpha_p)^\top$, with α_{p+1} capturing the direct effect of exposure A_i on the outcome Y_i .

Key features of these observed data models are: 1) Each mediator is modeled marginally (i.e., without influencing each other), and in the outcome model, mediators are linearly connected without interactions, which aligns with the structure required to estimate the mediation effect through independent pathways, as assumed in Figure 2; and 2) the use of a multivariate mediator model effectively captures the correlated nature of high-dimensional mediators.

2.2 Identifying assumptions

Linking potential outcomes to observed data requires additional assumptions beyond the SUTVA. While certain potential outcomes can be identified under SUTVA, outcomes involving multiple exposure levels represent unobservable quantities that cannot be identified from observed data without further assumptions.

To address the identification of such unobservable quantities, we used the assumption of causally independent mediators as proposed by [Imai and Yamamoto \(2013\)](#). In brief, this assumption states that each mediator is independent of the potential outcome, given

the confounders. For further details, refer to [Imai and Yamamoto \(2013\)](#). This assumption enables the nonparametric identification of each $IE_j(a, a')$, as well as the overall indirect effect $IE(a, a')$ and the direct effect $DE(a, a')$ for any two different exposure levels a and a' . Building on the observed data model from Section 2.1, the mediation effect through the j -th mediator is redefined as $IE_j(a, a') = (a - a')\delta_j\tau_j$. Moreover, the sum of all indirect effects and the direct effect are represented as $IE(a, a') = (a - a')\sum_{j=1}^q \delta_j\tau_j$ and $DE(a, a') = \alpha_{p+1}(a - a')$.

3 Bayesian Variable Selection

In this section, we present prior distributions, including a novel multivariate prior for the variable selection indicators, specially designed to leverage the dependence structure among mediators in a high-dimensional mediation analysis framework. We also address potential practical challenges, such as specifying a key hyperparameter and selecting appropriate thresholding for variable selection, along with their corresponding solutions. Details of the computational algorithm are provided in Supplementary Materials A.

3.1 Prior Distributions

The proposed Bayesian framework requires specification of prior distributions for the unknown model parameters. For automated variable selection, we employ spike-and-slab priors for the regression parameters $\boldsymbol{\tau}$ in the mediator model and $\boldsymbol{\delta}$ in the outcome model ([George and McCulloch, 1993, 1997](#)). Specifically, following priors are considered for τ_j and

$\delta_j, j = 1, \dots, q$:

$$\begin{aligned}\tau_j | \gamma_j, \Sigma &\sim \gamma_j \text{Normal}(0, v_j^2 \Sigma_{(j,j)}) + (1 - \gamma_j) I_0, \\ \delta_j | \omega_j, \sigma^2 &\sim \omega_j \text{Normal}(0, \psi_j^2 \sigma^2) + (1 - \omega_j) I_0,\end{aligned}\tag{3}$$

where γ_j and ω_j are binary latent variables that determine the membership of τ_j and δ_j to one of the components in the mixture distribution in the priors, respectively. v_j^2 and ψ_j^2 are the hyperparameters to specify. The exposure is considered to have a causal pathway to the j -th mediator if the data support $\gamma_j = 1$ over $\gamma_j = 0$. A similar interpretation holds for δ_j in the outcome model.

Independent and marginal Bernoulli priors are typically assumed for the latent binary variables γ_j and ω_j . However, use of the independent priors is less appealing in the mediation analysis in that, i) the information on the within-subject correlations among mediators in the data will not be utilized in variable selection in (1), despite the possibility that highly to moderately correlated mediators (see Figure 1) may be affected by the exposure; ii) variable selection will be performed separately in (1) and (2), leading to a subset of mediators with $\gamma_j = 0$ being unnecessarily tested in (2). To address these limitations, we propose an innovative approach for specifying priors for $(\boldsymbol{\gamma}, \boldsymbol{\omega})$ that integrate underlying dependence between mediators into the variable selection in (1), motivated by an MRF prior (Li and Zhang, 2010), and encourage the sequential selection of important intermediate variables from (1) for consideration in candidate mediators in (2), enabling more efficient and practical posterior simulations. Hereafter, we refer to these priors as MRF-SSB priors, with SSB representing sequential subsetting Bernoulli. Specifically, the conditional representation of the MRF-SSB priors is given by

$$\begin{aligned}\pi(\gamma_j | \boldsymbol{\gamma}_{(-j)}, \Sigma) &= p_j(\boldsymbol{\gamma}, \Sigma)^{\gamma_j} \{1 - p_j(\boldsymbol{\gamma}, \Sigma)\}^{1 - \gamma_j}, \\ \pi(\omega_j) &= \tilde{\gamma}_j \theta_\omega^{\omega_j} (1 - \theta_\omega)^{1 - \omega_j} + (1 - \tilde{\gamma}_j) I_0,\end{aligned}$$

where $\boldsymbol{\gamma}_{(-j)}$ is the vector $\boldsymbol{\gamma}$ with the j -th element removed, $\tilde{\gamma}_j$ denotes the value of γ_j , and

$$p_j(\boldsymbol{\gamma}, \Sigma) = \left\{ 1 + \exp \left(-\theta_\gamma - \eta \sum_{r \neq j} |c_{r,j}| \gamma_r \right) \right\}^{-1}.$$

$c_{r,j}$ is the correlation between the r -th and j -th mediators, calculated from Σ . It is noted that the SSB prior is conditional on the value $\tilde{\gamma}_j$, instead of the parameter γ_j , highlighting the “sequential subsetting” procedure, which forms candidate mediators for consideration in the selection of mediator-outcome causal pathways, receives feedback solely from the exposure-mediator model, but not vice versa. This approach is similar to the cutting feedback method proposed by [Lunn et al. \(2009\)](#). While the posterior distribution is constructed through correct decomposition of model parameters, the posterior updating process for $\boldsymbol{\gamma}$ does not incorporate the full conditional distribution.

The hyperparameter θ_γ controls the shrinkage of the model together with v_j^2 in (3). The hyperparameter η determines the extent to which other mediators, for a given mediator, impact the probability of including the exposure in the model (1). We note that setting $\eta=0$ leads to $\pi(\gamma_j | \boldsymbol{\gamma}_{(-j)}, \Sigma)$ being equivalent to the conventional independent Bernoulli (IB) prior for $\boldsymbol{\gamma}$. The hyperparameter θ_ω represents the initial guess for the proportion of mediating variables in the outcome model. We assign $\boldsymbol{\beta}_0 \sim \text{MVN}(0, h_0 I_q)$, $\boldsymbol{\beta}_j \sim \text{MVN}(0, c_0 I_p)$, $\alpha_0 \sim \text{Normal}(0, s_0)$, $\boldsymbol{\alpha} \sim \text{MVN}(0, t_0 I_p)$, and $\alpha_{p+1} \sim \text{Normal}(0, k_0)$. Lastly, we use the conjugate hyperpriors inverse-Gamma($\nu_0/2, \nu_0 \sigma_0^2/2$) and inverse-Gamma($\nu_1/2, \nu_1 \sigma_1^2/2$), for σ_Σ^2 and σ^2 , respectively. $(h_0, c_0, s_0, t_0, k_0, \nu_0, \sigma_0^2, \nu_1, \sigma_1^2)$ are the hyperparameters to be specified.

3.2 Practical considerations: phase transition and selection of variables

The Markov property of the proposed MRF-SSB priors is both conceptually and computationally advantageous, as it facilitates the characterization of the dependence structure among high-dimensional mediators. However, careful attention is required when setting values of (η, θ_γ) , since even small increases in these hyperparameters can significantly shift the size of the mediator model $(\sum_{j=1}^q \gamma_j)$, a phenomenon known as *phase transition* for MRF priors (Li and Zhang, 2010).

To specify η for a given value of θ_γ , Stingo et al. (2011) employ prior simulations over a grid of η values to identify the phase transition boundary, denoted as η_{pt} . A Beta prior is then placed on the ratio η/η_{pt} . In this work, we adopt a modified version of the posterior simulation approach, as demonstrated by Lee et al. (2017), which effectively addresses the relative underestimation of η_{pt} in the prior simulation method. Specifically, we run the following algorithm to detect η_{pt} over the posterior simulations: i) Simulate M_{pt} posterior samples for model parameters over a grid of η values, $\{\eta^g : g = 0, \dots, G, \eta^0 = 0\}$; ii) Let $\gamma_{(\eta^g)}$ denote the 50-th percentile of the posterior mean estimates of γ across mediators for the model (1) with $\eta = \eta^g$. Calculate $\gamma_{(\eta^g)}$ for $g = 0, \dots, G$; iii) Identify the phase transition value η_{pt} as η^g if $\gamma_{(\eta^g)} - \gamma_{(\eta^0)} > 0.05$; iv) Set $\eta = \eta^{g-1}$ in the proposed model.

Posterior inference for variable selection can be performed either through the joint posterior distribution of (γ, ω) , or via marginal posterior probabilities of inclusion (PPI) of the latent parameters. In our framework, We adopt the latter. Specifically, the indirect effect through mediator j is considered significant if the corresponding PPI exceeds a threshold κ , i.e., $\text{PPI}_j = P(\gamma_j = 1, \omega_j = 1 | \mathcal{D}) > \kappa$. A commonly used cutoff value of $\kappa = 0.5$ represents the median probability model. Given the sensitivity of this approach to the choice of $(\theta_\gamma,$

θ_ω), we implement an adaptive thresholding method from [Wadsworth et al. \(2017\)](#), where κ is selected to control the Bayesian false discovery rate (FDR). Specifically, we find an optimal value of κ such that $\text{FDR}(\kappa)$ is less than a pre-specified Bayesian FDR value (e.g. 0.05), where $\text{FDR}(\kappa) = \sum_{j=1}^q (1 - \text{PPI}_j) * I(\text{PPI}_j > \kappa) / \{\sum_{s=1}^q I(\text{PPI}_s > \kappa)\}$.

3.3 Computational Scheme

We develop a computationally efficient algorithm based on the covariance structure of a factor analytic (FA) model ([Hogan and Tchernis, 2004](#)), defined as $\Sigma = \sigma_\Sigma^2(\boldsymbol{\lambda}\boldsymbol{\lambda}^\top + I_q)$, where $\boldsymbol{\lambda} = (\lambda_1, \dots, \lambda_q)^\top$ is a $q \times 1$ vector of factor loadings. We assume a $\text{Normal}(\mu_\lambda, h_\lambda \sigma_\Sigma^2 I_q)$ prior with hyperparameters (μ_λ, h_λ) for each λ_j 's. Although this FA covariance model is relatively restrictive, it ensures computational feasibility for high-dimensional data in the proposed mediation analysis framework. Moreover, when used for the multivariate variable selection method with the MRF prior, the FA model demonstrates considerable robustness even in cases when Σ is misspecified ([Lee et al., 2017](#)). In Section 4, we examine the performance of our variable selection method under model misspecification scenarios.

Estimation and inference for the proposed framework are performed based on samples from the joint posterior distribution by either exploiting prior-posterior conjugacies or using the adaptive Metropolis-Hastings algorithm. To improve the convergence of the stochastic search variable selection (SSVS) steps for updating $\boldsymbol{\tau}$ and $\boldsymbol{\delta}$, we introduce “refinement” steps, where the non-zero elements of the parameters are further updated via the Gibbs sampler. This refined SSVS algorithm shows substantially enhanced mixing of MCMC chains in our numerical studies, leading to improved computational performance. A detailed description of the proposed computational scheme is provided in Supplementary Materials A. To increase the computation speed, we develop a series of core functions in C++. The algorithm is publicly available on the first author’s GitHub page

(<https://github.com/YounghoBae/BVSMed>). It takes approximately 30 minutes to run 10,000 MCMC iterations on a 3.2 GHz Apple M1 MacBook Pro for the analysis of the metabolomics data from MBS/MLVS ($n=466$, $q=298$, $p=3$).

4 Simulation Studies

In this section, we present simulation studies to assess the performance of the proposed framework in variable selection and estimation across a range of scenarios. The primary goal is to compare the proposed MRF-SSB prior with its standard counterpart in mediation analysis involving high-dimensional mediators. Specifically, we investigate how performance varies with the magnitude of indirect effects, the correlation structure among mediators, and the impact of misspecification of covariance structures.

4.1 Set-up and data generation

We considered the four different scenarios. In Scenarios I-III, we generated samples of size $n = 1,000$, with $q = 300$ mediators and $p = 5$ confounders under the proposed model outlined in Sections 2 and 3. Each scenario assumes different level and structure of correlation among mediators by varying $\boldsymbol{\lambda}$. Specifically, $\boldsymbol{\lambda} = 0.35 \cdot \mathbf{1}_q$ induced a correlation of 0.1 among mediators in Scenario I and III, while independent mediators were assumed with $\boldsymbol{\lambda} = \mathbf{0}_q$ in Scenario II. In Scenario IV, we matched the data dimensions with those from the NHSII/HPFS ($n = 466$, $q = 298$, $p = 3$), and set Σ to the sample covariance matrix estimated from the data, representing a case of misspecified covariance structure.

In all four scenarios, confounders (\mathbf{X}) were independently generated from a $\text{Normal}(0, 1)$, while the exposure was assumed to follow a $\text{Normal}(\mathbf{l}^\top \mathbf{X}, 1)$, where $\mathbf{l} = (0.5, 0.2, 0.7, 0.4, 0.6)^\top$ for Scenarios I-III and $\mathbf{l} = (0.5, 0.2, 0.7)^\top$ for Scenario IV. This setting indicates that the

outcome and exposure are confounded by \mathbf{X} .

The parameters regulating the effect sizes of the exposure-mediator pathways and the mediator-outcome pathways, were set as $\boldsymbol{\tau} = (-0.12 \cdot \mathbf{1}_5, -0.08 \cdot \mathbf{1}_5, -0.04 \cdot \mathbf{1}_5, 0.04 \cdot \mathbf{1}_5, 0.08 \cdot \mathbf{1}_5, 0.12 \cdot \mathbf{1}_5, \mathbf{0}_{q-30})^\top$ and $\boldsymbol{\delta} = (\mathbf{d} \otimes \mathbf{1}_6, \mathbf{0}_{q-30})^\top$, where $\mathbf{d} = (0.5, 1.0, 1.5, 0, 0)^\top$ in Scenarios I, II, and IV. It is noted that, in Scenario IV, we rearranged the elements of Σ so that highly correlated mediators ($\text{corr} > 0.6$) are aligned with the first 30 exposure-mediator pathways in this data-generating mechanism. We considered the *null* case by setting all elements of $\boldsymbol{\tau}$ to zero, indicating no active pathways, in Scenario III. Finally, we set $\boldsymbol{\beta}_0 = 0.1 \cdot \mathbf{1}_q$, $\mathbf{B} = 0.1 \cdot \mathbf{1}_{p \times q}$, and $\sigma_\Sigma^2 = 0.5$ in the mediator model (1), and $\alpha_0 = 2$, $\boldsymbol{\alpha} = 2 \cdot \mathbf{1}_p$, $\sigma^2 = 0.5$, and $\alpha_{p+1} = 2$ in the outcome model (2).

4.2 Specification of hyperparameters and analysis settings

We fitted three different models to 480 simulated datasets, 120 under each of the four scenarios. The models are the proposed MVN-MRF-SSB, and two competing models, Normal-IB-SSB and MVN-IB-SSB. These models represent different combinations of underlying mediator models (MVN or independent Normals) and priors for selection indicators in the mediator model (MRF or IB) and the outcome model (SSB). The simplest of the three, Normal-IB-SSB, assumes no correlation among mediators, similar to the approach by Song et al. (2020). In contrast, MVN-IB-SSB explicitly models the correlation structure among the mediators, providing more flexibility, but it is limited in that it does not fully exploit the dependence of mediators in pathway identification, as it employs simple IB priors for selection indicator parameters.

As outlined in Section 3, the proposed Bayesian framework requires the specification of hyperparameters. The hyperparameters were set as $(h_0, c_0, s_0, t_0, k_0, h_\lambda) = 100$, $(\mu_0, \mu_1, \mu_\lambda) = 0$, $(\nu_0, \nu_1) = 6$, $(\sigma_0^2, \sigma_1^2) = 1/3$, to make the corresponding priors relatively

non-informative. We set $\text{logit}^{-1}(\theta_\gamma) = \theta_\omega = 0.1$, indicating prior probabilities of 0.1 for both the association between the exposure and mediators in (1) and the association between mediators and the outcome in (2). Finally, $v_j^2 = \psi_j^2 = 9$, and the value of η for the proposed MVN-MRF-SSB was selected based on the posterior simulation approach introduced in Section 3.2. For Scenarios I-III, we ran each MCMC chain for 150,000 iterations, using the first half as burn-in. In Scenario IV, where the models may require additional iterations to adequately adapt to the complex underlying correlation structure and smaller sample size setting, we increased the total number of iterations to 300,000. We assessed model convergence via visual inspection of trace plots and further confirmed it by calculating the Gelman-Rubin potential scale reduction (PSR) statistic (Gelman et al., 2013) for representative model parameters.

We evaluated the performance of the variable selection feature of the models using five quantities: true positive rate (TPR), false positive rate (FPR), negative predictive value (NPV), positive predictive value (PPV), and the number of variables selected (NVS). The indirect effect estimates were summarized as the median of the posterior means from 120 replicates for each scenario, with the corresponding standard deviations also provided.

4.3 Results

As aforementioned, the primary aim of our numerical studies was to evaluate the improvement achieved by the proposed MRF-SSB priors compared to a conventional counterpart. To this end, we presented the comparative analysis of the MVN-MRF-SSB model alongside the MVN-IB-SSB model in the main manuscript, allowing for an assessment of both models under identical conditions, differing only in their prior structures for γ . Results from Normal-IB-SSB are provided in Supplementary Materials B.2 for reference.

When the mediators were uncorrelated (Scenario II), both models exhibited nearly

Table 1: Four operating characteristics[†] (%) and the number of variables selected (NVS) for the exposure-mediator pathways (γ) and the combined exposure-mediator-outcome pathways ($\gamma \times \omega$) in the multivariate normal models with independent Bernoulli and sequential subsetting Bernoulli priors (MVN-IB-SSB) and the proposed Markov random field and sequential subsetting priors (MVN-MRF-SSB) across four simulation scenarios described in Section 4.1.

Scenario		MVN-IB-SSB				MVN-MRF-SSB			
		γ		$\gamma \times \omega$		γ		$\gamma \times \omega$	
		Mean	(SD)	Mean	(SD)	Mean	(SD)	Mean	(SD)
I	TPR	58.4	(5.3)	56.9	(7.3)	68.7	(5.9)	68.1	(7.7)
	FPR	0.3	(0.3)	1.6	(0.5)	1.4	(0.8)	0.7	(0.4)
	PPV	95.8	(4.1)	70.1	(8.2)	84.7	(7.0)	86.9	(8.1)
	NPV	95.6	(0.5)	97.3	(0.5)	96.6	(0.6)	98.0	(0.5)
	NVS	18.3	(1.7)	14.7	(1.6)	24.5	(2.9)	14.1	(1.2)
II	TPR	59.8	(5.6)	58.9	(7.4)	59.8	(5.2)	58.9	(7.2)
	FPR	0.2	(0.3)	0.0	(0.1)	0.3	(0.3)	0.0	(0.1)
	PPV	96.6	(3.9)	98.9	(3.0)	96.3	(4.1)	99.0	(2.8)
	NPV	95.7	(0.6)	97.4	(0.4)	95.7	(0.5)	97.4	(0.4)
	NVS	18.6	(1.7)	10.7	(1.4)	18.6	(1.6)	10.7	(1.3)
III [‡]	TPR	–	–	–	–	–	–	–	–
	FPR	0.1	(0.2)	0.1	(0.2)	0.1	(0.2)	0.1	(0.2)
	PPV	–	–	–	–	–	–	–	–
	NPV	100.0	(0.0)	100.0	(0.0)	100.0	(0.0)	100.0	(0.0)
	NVS	0.4	(0.7)	0.4	(0.7)	0.4	(0.7)	0.4	(0.7)
IV	TPR	24.1	(9.0)	13.2	(9.6)	45.2	(12.7)	21.9	(12.4)
	FPR	0.3	(0.4)	0.3	(0.3)	0.7	(1.6)	0.2	(0.2)
	PPV	92.5	(10.8)	75.3	(27.6)	91.2	(11.8)	90.9	(13.3)
	NPV	92.2	(0.9)	94.7	(0.6)	94.2	(1.3)	95.2	(0.7)
	NVS	7.9	(3.1)	3.2	(2.3)	15.4	(6.8)	4.4	(2.4)

NOTE: Throughout values are based on results from 120 simulated datasets.

[†] true positive rate (TPR), false positive rate (FPR), negative predictive value (NPV), and positive predictive value (PPV)

[‡] TPR and PPV are not presented, as there are no active pathways.

Table 2: Estimated indirect effects (IEs)[†] and marginal posterior probabilities of inclusion (PPI) for the multivariate normal models with independent Bernoulli and sequential subsetting Bernoulli priors (MVN-IB-SSB) and the proposed Markov random field and sequential subsetting priors (MVN-MRF-SSB) for Scenario I. Estimated direct effect (DE)[†] is also provided.

j	True			MVN-IB-SSB		MVN-MRF-SSB		j	True			MVN-IB-SSB		MVN-MRF-SSB	
	τ_j	δ_j	IE_j	IE_j^{\ddagger}		IE_j			τ_j	δ_j	IE_j	IE_j		IE_j	
				PM (SD)	\overline{PPI}	PM (SD)	\overline{PPI}					PM (SD)	\overline{PPI}	PM (SD)	\overline{PPI}
1	-0.12	0.5	-0.12	-0.19 (0.05)	0.98	-0.16 (0.04)	0.99	16	0.04	0.5	0.04	0.08 (0.04)	0.14	0.06 (0.04)	0.31
2	-0.12	1.0	-0.24	-0.32 (0.07)	0.98	-0.29 (0.06)	0.99	17	0.04	1.0	0.08	0.13 (0.05)	0.08	0.10 (0.06)	0.26
3	-0.12	1.5	-0.36	-0.44 (0.09)	1.00	-0.40 (0.08)	1.00	18	0.04	1.5	0.12	0.17 (0.08)	0.07	0.13 (0.08)	0.18
4	-0.12	0.0	0.00	-0.06 (0.03)	0.65	-0.05 (0.02)	0.14	19	0.04	0.0	0.00	0.03 (0.02)	0.05	0.02 (0.01)	0.05
5	-0.12	0.0	0.00	-0.06 (0.04)	0.61	-0.04 (0.03)	0.15	20	0.04	0.0	0.00	0.03 (0.02)	0.10	0.02 (0.01)	0.06
6	-0.08	0.5	-0.08	-0.13 (0.04)	0.68	-0.11 (0.04)	0.80	21	0.08	0.5	0.08	0.12 (0.04)	0.54	0.10 (0.03)	0.81
7	-0.08	1.0	-0.16	-0.20 (0.06)	0.65	-0.19 (0.05)	0.82	22	0.08	1.0	0.16	0.21 (0.07)	0.70	0.19 (0.06)	0.85
8	-0.08	1.5	-0.24	-0.29 (0.08)	0.67	-0.28 (0.08)	0.81	23	0.08	1.5	0.24	0.29 (0.09)	0.62	0.28 (0.08)	0.83
9	-0.08	0.0	0.00	-0.04 (0.02)	0.34	-0.03 (0.02)	0.11	24	0.08	0.0	0.00	0.04 (0.02)	0.37	0.03 (0.02)	0.18
10	-0.08	0.0	0.00	-0.05 (0.02)	0.37	-0.03 (0.02)	0.18	25	0.08	0.0	0.00	0.04 (0.02)	0.38	0.03 (0.02)	0.21
11	-0.04	0.5	-0.04	-0.07 (0.04)	0.10	-0.05 (0.03)	0.20	26	0.12	0.5	0.12	0.19 (0.05)	0.98	0.16 (0.04)	0.99
12	-0.04	1.0	-0.08	-0.12 (0.06)	0.07	-0.10 (0.05)	0.23	27	0.12	1.0	0.24	0.31 (0.07)	0.98	0.29 (0.06)	1.00
13	-0.04	1.5	-0.12	-0.17 (0.09)	0.04	-0.14 (0.08)	0.19	28	0.12	1.5	0.36	0.43 (0.09)	0.97	0.40 (0.08)	0.99
14	-0.04	0.0	0.00	-0.03 (0.02)	0.02	-0.02 (0.01)	0.03	29	0.12	0.0	0.00	0.07 (0.03)	0.66	0.05 (0.02)	0.15
15	-0.04	0.0	0.00	-0.03 (0.02)	0.06	-0.02 (0.01)	0.05	30	0.12	0.0	0.00	0.07 (0.03)	0.59	0.04 (0.03)	0.16
	True			DE*		DE			True			DE		DE	
	DE			PM (SD)		PM (SD)			DE			PM (SD)		PM (SD)	
	4.00			3.99 (0.25)		4.00 (0.19)			4.00			3.99 (0.25)		4.00 (0.19)	

NOTE: Throughout values are based on results from 120 simulated datasets.

Results are shown for the first 30 mediators ($j = 1, \dots, 30$) that are causally affected by the exposure.

[†] IE: indirect effect, defined as $2\tau\delta$, DE: direct effect, defined as $2\alpha_{p+1}$. The value “2” represents the difference between two exposure levels, which correspond to the 25th and 75th percentiles of the exposure distribution.

[‡] The medians of the posterior means (PM) and posterior standard deviation (SD) of IE_j conditioning on $\gamma_j = 1$ and $\omega_j = 1$, the medians of the posterior means of PPI ($\gamma_j \times \omega_j$) are computed.

* The medians of the posterior means (PM) and posterior standard deviation (SD) of DE are computed.

identical variable selection performance (Table 1). However, in scenarios with correlated mediators and active pathways (I, IV), the proposed MVN-MRF-SSB model outperformed the MVN-IB-SSB model in sensitivity. For example, in Scenario I, the MVN-MRF-SSB achieved a TPR of 68%, compared to 57% for the MVN-IB-SSB, in detecting exposure-mediator-outcome pathways ($\gamma \times \omega$). This difference is further illustrated in the estimated indirect effects (IEs) presented in Table 2. Both models successfully identified the IEs involving the six largest exposure-mediator effects ($|\tau_j| = 0.12$). However, the MVN-MRF-SSB performed much better at detecting IEs linked to smaller-magnitude exposure-mediator associations, yielding PPIs greater than 0.80, in contrast to 0.70 or less for the competing model, for mediators 6-8 and 21-23, where $|\tau_j| = 0.08$. Thus, this improved performance was attributed to the MRF prior’s ability to identify exposure-mediator pathways (TPR of 69% compared to 58% with the IB priors, see Table 1 for γ) by effectively exploiting mediator correlations.

When n was smaller and the covariance model was misspecified (Scenario IV), the overall sensitivity for detecting causal pathways, which were held constant across scenarios, decreased as expected. However, the ability to detect exposure-mediator pathways improved more significantly (44% versus 22% for γ) due to the inclusion of stronger correlations among relevant mediators (>0.6) in the MRF prior. This improvement resulted in greater power to identify active mediating pathways (19% versus 11% for $\gamma \times \omega$).

The proposed model achieved the same level of specificity or better when compared to the competing model. In the null case (Scenario III), both models successfully excluded inactive pathways, even with the presence of correlated mediators. In Scenarios I and IV, however, the proposed MRF prior identified more relevant candidate exposure-mediator pathways than the IB priors, although it slightly increased the FPR (1.4% versus 0.3% and 0.6% versus 0.2%, respectively; see Table 1). Then, the sparsity property of the proposed

SSB priors encouraged the exclusion of irrelevant pathways in the outcome model, resulting in a lower FPR for the final quantities of interest, indirect effects, in the MVN-MRF-SSB model (0.7% versus 1.6% and 0.1% versus 0.2%, respectively; see Table 1).

In the estimation of active pathways (Table 2), when the indirect effect size was large (e.g., IE_j for $j = 1, 2, 3$), the proposed MVN-MRF-SSB produced effect estimates closest to the true values, while the competing model overestimated the effect magnitudes. Additionally, as the indirect effect size increased, the estimated PPI from the proposed model approached 1, indicating a high level of confidence in selecting active mediation pathways. In cases with null indirect effects (e.g., IE_j for $j = 4, 5$), the competing model provided effect estimates further from zero than the proposed model, and the corresponding PPIs were estimated to be closer to 1. When the indirect effect sizes were similar (e.g., for the pairs $j = 2$ and $j = 8$ or $j = 1$ and $j = 13$), decreasing τ led to increased bias and uncertainty in effect estimation in the competing model, along with a lower average estimated PPI. However, the proposed model showed a smaller degree of bias and uncertainty compared to the competing model, particularly for moderate τ values (e.g., ± 0.08), where it maintained relatively high estimated PPIs. This further demonstrates that the variable selection method based on the MRF prior performs effectively, even for smaller τ values, resulting in more accurate indirect effect estimations. Estimates of active pathways for Scenarios II-IV are provided in Supplementary Materials B.1.

In summary, across all scenarios, our simulation studies highlighted the importance of accounting for correlations among mediators. The proposed method effectively addressed this challenge by integrating the correlation structure through a multivariate model and by incorporating mediator interdependence into the stochastic search variable selection process using MRF-SSB priors.

5 Application to Metabolomics Data

The Bayesian framework proposed in this research is motivated by the integration of epidemiological studies and blood biomarker analyses, aiming to investigate the relationship between long-term adherence to the Mediterranean diet and cardiometabolic health. Plasma metabolomes are explored as potential mediators of this relationship. The specific objectives of the research include the identification of metabolites that mediate the causal pathway between adherence to the Mediterranean diet and cardiometabolic outcomes and the estimation of the corresponding indirect effects.

5.1 Health Professionals Follow-up Study and Nurses' Health Study II

We applied the proposed variable selection method to data from $n = 466$ participants in the NHSII/HPFS substudies, including $q = 298$ plasma metabolites. The exposure of interest (A) was Alternate Mediterranean Diet score, inverse-normal transformed (mean=-0.02, s.d.=0.98), which reflects adherence to the Mediterranean Diet (Shan et al., 2023). The outcome (Y), a cardiometabolic disease risk score (mean=9.0, s.d.=2.7), was calculated by summing the level of three biomarkers associated with the pathogenesis of cardiometabolic disease, with higher scores indicating a high risk. Metabolites, the potential mediators (\mathbf{M}), with high skewness (absolute skewness >2) were log-transformed, and all metabolites were standardized to z -scores within each substudy (Kim, 2013). Missing metabolite data were imputed using the random forest imputation method (Wei et al., 2018). Additional details of the data collection and processing are provided in Supplementary Materials C.

5.2 Specification of hyperparameters and analysis settings

We fitted the proposed MVN-MRF-SSB and two competing models, MVN-IB-SSB and Normal-IB-SSB, to the HPFS/NHSII data. In our analyses, we included age (mean=66.7, s.d.=6.5), sex (0=male: 56.4%; 1=female: 43.6%), and body mass index (BMI, mean=26.0, s.d.=4.8 kg/m²) as covariates (\mathbf{X} , $p = 3$) without performing variable selection on them. Hyperparameters for all models were set to the same values as in Section 4.2. Three independent MCMC chains were run for a total of 300,000 iterations each, with the first half discarded as burn-in. Convergence was assessed by inspection of trace plots as well as calculation of the PSR statistic, requiring PSR values below 1.05 for model parameters.

5.3 Results

As in the simulation studies, the main paper presented results from the proposed MVN-MRF-SSB model and the competing MVN-IB-SSB model. Results from the Normal-IB-SSB model were provided in Supplementary Materials D. We also provided overlaid trace plots for the illustrative parameters ($\boldsymbol{\lambda}$, $\boldsymbol{\delta}$) in the proposed model, which exhibited the slowest convergence among all model parameters, in Table D.2 and D.3. The plots indicated that the chains mixed well and converged early in the iterations, suggesting that, in practice, 300,000 iterations were not necessary for fitting our proposed model.

We applied a PPI cutoff of κ for variable selection, estimated using the adaptive thresholding approach described in Section 3.2. The estimated inclusion probabilities for selected pathways, along with their corresponding metabolite mediators, were presented in Figure 3. Among the 298 potential pathways, the competing method identified a total of 8 pathways. In contrast, the proposed MVN-MRF-SSB selected 7 additional pathways, highlighting 15 metabolites that may play an important intermediate role in the causal pathway between

Table 3: Estimated indirect effects (IEs)[†] of adherence to the Mediterranean diet on cardiometabolic disease risk through active pathways identified by multivariate normal models with independent Bernoulli and sequential subsetting Bernoulli priors (MVN-IB-SSB) and the proposed Markov random field and sequential subsetting priors (MVN-MRF-SSB). Estimated effects of diet on metabolites (τ) are also provided.

Metabolites [‡]	MVN-IB-SSB		MVN-MRF-SSB	
	τ	IE	τ	IE
	PM (95% HPDI)*	PM (95% HPDI)**	PM (95% HPDI)*	PM (95% HPDI)**
C53:2 TG	-	-	-0.22 (-0.26, 0.00)	-0.22 (-0.35, 0.00)
C51:3 TG	-	-	-0.25 (-0.30, -0.21)	0.15 (0.00, 0.25)
C51:2 TG	-0.25 (-0.30, 0.00)	0.20 (-0.15, 0.47)	-0.25 (-0.30, -0.20)	0.42 (0.00, 0.71)
C51:1 TG	-0.25 (-0.28, 0.00)	-0.21 (-0.31, 0.00)	-0.24 (-0.30, -0.19)	-0.24 (-0.38, 0.00)
C50:4 TG	-	-	-0.21 (-0.24, 0.00)	-0.22 (-0.38, 0.00)
C50:3 TG	-0.23 (-0.27, 0.00)	-0.39 (-0.51, 0.00)	-0.24 (-0.28, -0.18)	-0.35 (-0.51, 0.00)
C49:3 TG	-0.29 (-0.34, -0.24)	0.11 (-0.23, 0.43)	-0.29 (-0.33, -0.24)	0.30 (0.00, 0.48)
C38:4 GPC	-0.27 (-0.31, -0.22)	0.11 (-0.09, 0.22)	-0.27 (-0.32, -0.23)	0.13 (0.00, 0.22)
C34:0 PS	0.14 (0.00, 0.18)	0.09 (0.00, 0.15)	0.14 (0.00, 0.18)	0.08 (0.00, 0.12)
C22:6 LPC	-	-	0.18 (0.13, 0.22)	-0.08 (-0.13, 0.00)
C22:6 CE	-	-	0.22 (0.17, 0.27)	0.16 (0.00, 0.26)
C20:5 LPC	0.17 (0.12, 0.21)	-0.12 (-0.18, 0.00)	0.17 (0.12, 0.21)	-0.11 (-0.16, 0.00)
C20:5 CE	-	-	0.20 (0.16, 0.24)	0.10 (0.00, 0.16)
C18:1 SM	-	-	-0.16 (-0.20, 0.00)	-0.06 (-0.08, 0.00)
C18:0 CE	-0.16 (-0.20, 0.00)	-0.19 (-0.24, 0.00)	-0.16 (-0.20, 0.00)	-0.18 (-0.23, 0.00)

NOTE: We adjusted for participants' age, sex, and body mass index, potential confounders, but did not perform variable selection on them.

[†] IE: indirect effect, defined as $1.03\tau\delta$. The value "1.03" represents the difference between two exposure levels, which correspond to the 30th and 70th percentiles of the exposure distribution.

[‡] CE: cholesterol, TG: triacylglycerol, LPC: lysophosphatidylcholine, GPC: glycerophospholipid, SM: sphingomyelin,

PS: phosphatidylserine

* Posterior median (PM) of τ (conditioning on $\gamma = 1$) and 95% highest posterior density intervals (HPDI) for τ

** Posterior median (PM) of $1.03\tau\delta$ (conditioning on $\gamma = 1, \omega = 1$) and 95% highest posterior density intervals (HPDI) for $1.03\tau\delta$

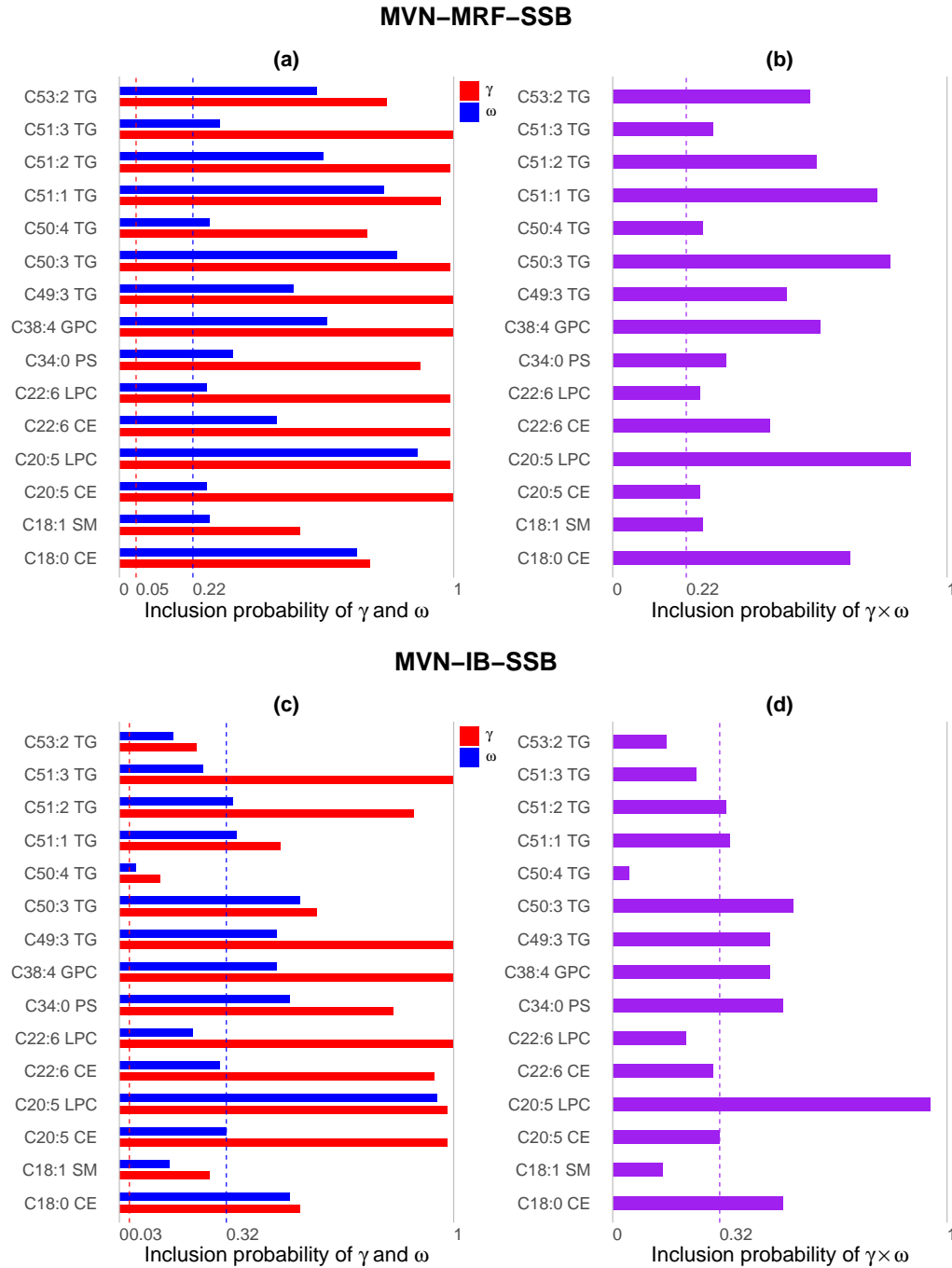


Figure 3: Estimated marginal posterior probabilities of inclusion (PPI) associated with the indirect effects of adherence to the Mediterranean diet on cardiometabolic disease risk, estimated by multivariate normal models with independent Bernoulli and sequential subsetting Bernoulli priors (MVN-IB-SSB) and the proposed Markov random field and sequential subsetting priors (MVN-MRF-SSB). The vertical line represents the cutoff value κ for variable selection, as determined by the adaptive thresholding method described in Section 3.2.

the Mediterranean diet and cardiometabolic disease risk. These results were attributed to the MRF-SSB priors devised for the proposed framework. As stated in Sections 3.1 and 4.3, the MRF prior first improved the ability to identify subtle effects of exposure on a metabolite measure when other correlated metabolites were also affected by the exposure. This was evident when comparing the PPI of γ for the two models, as shown in Figure 3(a) and 3(c). Subsequently, the SSB prior finalized the selection of the active pathways (Figure 3(b) and 3(d)).

We provided estimated indirect effects and associated uncertainties as posterior medians (PM) and 95% highest posterior density intervals (HPDI) in Table 3. The two exposure levels (a and a') for analyzing the effect were set at -0.54 and 0.49, corresponding to the 30th and 70th percentiles of the exposure, Alternative Mediterranean Diet score. Therefore, the j -th indirect effect IE_j to be estimated is $1.03\tau_j\delta_j$, and the direct effect is $1.03\alpha_{p+1}$. The indirect effect estimates for identified pathways ranged from -0.35 to 0.42 in the MVN-MRF-SSB model, compared to a range of -0.39 to 0.21 in the MVN-IB-SSB model. Among the metabolites selected by both models, C51:2 triacylglycerols (TG) and C49:3 TG exhibited stronger indirect effects in the MVN-MRF-SSB model (PM: 0.42 and 0.30, respectively) than in the MVN-IB-SSB model (PM: 0.20 and 0.11, respectively). The estimated uncertainties, as indicated by the width of the HPDI, were largely comparable across the pathways identified by both models. The estimated direct effect was similar between the two models: PM (95% HPDI) was -0.12 (-0.34, 0.11) for the MVN-MRF-SSB model and -0.14 (-0.35, 0.11) for the MVN-IB-SSB model.

The results were consistent with previous studies that have shown protective indirect effects of the Mediterranean diet on cardiometabolic disease risk through several specific metabolites. For example, both models identified C20:5 lysophosphatidylcholine (LPC) (Table 3), a well-established metabolic marker of fish intake, a key element of the Mediterranean

diet. However, another marker associated with fish intake—C22:6 LPC—was uniquely identified by the proposed MVN-MRF-SSB model. These metabolites, which were inversely associated with cardiometabolic disease risk, further supported the protective (negative) indirect effects of the Mediterranean diet on cardiometabolic health.

6 Discussion

In this paper, we introduced a novel Bayesian variable selection method for mediation analysis that accommodates the correlation structure of high-dimensional mediators through the priors of the selection indicators. We developed the special MRF-SSB priors to improve the power to detect active exposure-mediator-outcome pathways. The proposed mediation analysis approach allowed us to identify a subset of metabolites that mediate the relationship between adherence to a Mediterranean diet and cardiometabolic health outcomes while also enabling us to estimate and make inferences about the indirect effects associated with these metabolites. Notably, the proposed Bayesian framework identified a set of additional metabolites that were not detected by conventional Bayesian models using standard priors.

It is noted that, in practice, the estimated direct effects in our application may partially reflect effects mediated by other factors, such as filtered or unmeasured metabolites. Additionally, our data analyses were intended primarily as illustrative examples to highlight the potential advantages of the proposed method. Questions may arise regarding the analysis setup, as adjustments were made for only three confounders: age, sex, and BMI. We are currently investigating the performance of the methods across various model setups, including those with more comprehensive confounder adjustments.

Central to the proposed method is the incorporation of mediator correlations into the variable selection and the estimation of active pathways, which was shown to be effective

in our numerical studies. However, it is important to acknowledge two limitations. First, while the proposed method exploits the correlation structure among high-dimensional mediators, it does not account for the sequential order among them (i.e., cause-and-effect relationships). When such a sequential order exists, defining individual indirect effects and introducing the corresponding identifying assumptions becomes a challenging problem, even with a limited number of mediators (VanderWeele and Vansteelandt, 2014; Daniel et al., 2015). Extending this to high-dimensional mediators presents an additional topic for further research. One possible approach is to begin by estimating the directed acyclic graph (DAG) to identify active pathways (Castelletti, 2020), then calculate each mediation effect as the indirect effect remaining after accounting for earlier mediators in the sequential pathway order. However, DAG estimation is particularly challenging with high-dimensional mediators, and developing precise identifying assumptions for the inferred DAG adds further complexity to the process.

Second, the proposed model is based on the covariance structure of a FA model, which may be too restrictive for accurately capturing the complex dependencies among mediators in practice. Our simulation studies demonstrated improved performance of the proposed model, even when this structure was misspecified. Nevertheless, adopting more flexible covariance structures, such as the unstructured model or sparse infinite factor models (Bhattacharya and Dunson, 2011), could further enhance the model’s performance by leveraging the synergy between better-estimated correlations and the MRF-SSB priors. These extensions, however, require addressing computational challenges that must arise from estimating higher-dimensional models, such as consideration of regularization methods for sparse unstructured covariance models (Chu et al., 2013). The development of more computationally efficient algorithm for detecting phase transitions is also necessary to scale up the method (Zhao et al., 2024).

The proposed MRF-SSB priors can be adopted to mediation models with various types of mediators and outcomes. For non-continuous mediators, such as binary, categorical, or count data, generalized linear models can be incorporated into the mediator model. We are currently extending the framework to handle discrete and time-to-event outcomes, which are crucial for analyzing commonly observed outcomes in integrated epidemiological studies, such as disease status and time to diagnosis or death. These extensions are expected to improve the framework's applicability in medical and epidemiological research by accommodating more complex data types.

In conclusion, the proposed Bayesian framework provides researchers with more powerful statistical tools to identify active pathways and estimate their associated effects in mediation analysis. The methods developed in this research along with publicly available software and insights from our numerical studies will benefit a wide range of fields beyond metabolomics study, particularly in contexts involving correlated continuous mediators.

Funding

This work was supported by the National Institute of Dental and Craniofacial Research of USA (R03DE027486), the National Institute of General Medical Sciences of USA (R01GM126257) and the National Research Foundation (NRF) grant of South Korea (NRF-2020R1F1A1A01048168, NRF-2022R1F1A1062904, RS-2024-00407300). The Health Professionals Follow-Up study and Nurse's Health Study were supported by the National Cancer Institute of USA (U01CA167552, U01CA176726).

References

- Aung, M. T., Song, Y., Ferguson, K. K., Cantonwine, D. E., Zeng, L., McElrath, T. F., Pennathur, S., Meeker, J. D., and Mukherjee, B. (2020). Application of an analytical framework for multivariate mediation analysis of environmental data. *Nature Communications*, 11(1):5624.
- Bao, Y., Bertoina, M. L., Lenart, E. B., Stampfer, M. J., Willett, W. C., Speizer, F. E., and Chavarro, J. E. (2016). Origin, methods, and evolution of the three nurses' health studies. *American Journal of Public Health*, 106(9):1573–1581.
- Bhattacharya, A. and Dunson, D. B. (2011). Sparse Bayesian infinite factor models. *Biometrika*, 98(2):291–306.
- Breiman, L. and Friedman, J. (1997). Predicting multivariate responses in multiple linear regression. *Journal of the Royal Statistical Society: Series B*, 59(1):3–54.
- Castelletti, F. (2020). Bayesian model selection of Gaussian directed acyclic graph structures. *International Statistical Review*, 88(3):752–775.
- Chén, O. Y., Crainiceanu, C., Ogburn, E. L., Caffo, B. S., Wager, T. D., and Lindquist, M. A. (2018). High-dimensional multivariate mediation with application to neuroimaging data. *Biostatistics*, 19(2):121–136.
- Chu, H., Ibrahim, J. G., Khondker, Z. S., Lin, W., and Zhu, H. (2013). The Bayesian covariance lasso. *Statistics and its Interface*, 6(2):243–259.
- Daniel, R. M., De Stavola, B. L., Cousens, S. N., and Vansteelandt, S. (2015). Causal mediation analysis with multiple mediators. *Biometrics*, 71(1):1–14.

- Derkach, A., Pfeiffer, R. M., Chen, T.-H., and Sampson, J. N. (2019). High dimensional mediation analysis with latent variables. *Biometrics*, 75(3):745–756.
- Forastiere, L., Mealli, F., and VanderWeele, T. J. (2016). Identification and estimation of causal mechanisms in clustered encouragement designs: disentangling bed nets using Bayesian principal stratification. *Journal of the American Statistical Association*, 111(514):510–525.
- Gao, Y., Yang, H., Fang, R., Zhang, Y., Goode, E. L., and Cui, Y. (2019). Testing mediation effects in high-dimensional epigenetic studies. *Frontiers in genetics*, 10:1195.
- Gelman, A., Carlin, J. B., Stern, H. S., and Rubin, D. B. (2013). *Bayesian Data Analysis*. Chapman and Hall/CRC Boca Raton.
- George, E. and McCulloch, R. (1997). Approaches for Bayesian variable selection. *Statistica Sinica*, 7:339–374.
- George, E. I. and McCulloch, R. E. (1993). Variable selection via Gibbs sampling. *Journal of the American Statistical Association*, 88(423):881–889.
- Hogan, J. W. and Tchernis, R. (2004). Bayesian factor analysis for spatially correlated data, with application to summarizing area-level material deprivation from census data. *Journal of the American Statistical Association*, 99(466):314–324.
- Huang, T., Trudel-Fitzgerald, C., Poole, E. M., Sawyer, S., Kubzansky, L. D., Hankinson, S. E., Okereke, O. I., and Tworoger, S. S. (2019). The mind–body study: Study design and reproducibility and interrelationships of psychosocial factors in the nurses’ health study II. *Cancer Causes & Control*, 30:779–790.

- Huang, Y.-T. and Pan, W.-C. (2016). Hypothesis test of mediation effect in causal mediation model with high-dimensional continuous mediators. *Biometrics*, 72(2):402–413.
- Imai, K. and Yamamoto, T. (2013). Identification and sensitivity analysis for multiple causal mechanisms: Revisiting evidence from framing experiments. *Political Analysis*, 21(2):141–171.
- Kim, H.-Y. (2013). Statistical notes for clinical researchers: assessing normal distribution (2) using skewness and kurtosis. *Restorative Dentistry & Endodontics*, 38(1):52–54.
- Lee, K. H., Coull, B. A., Moscicki, A.-B., Paster, B. J., and Starr, J. R. (2020). Bayesian variable selection for multivariate zero-inflated models: Application to microbiome count data. *Biostatistics*, 21(3):499–517.
- Lee, K. H., Tadesse, M. G., Baccarelli, A. A., Schwartz, J., and Coull, B. A. (2017). Multivariate Bayesian variable selection exploiting dependence structure among outcomes: Application to air pollution effects on DNA methylation. *Biometrics*, 73(1):232–241.
- Li, F. and Zhang, N. (2010). Bayesian variable selection in structured high-dimensional covariate spaces with applications in genomics. *Journal of the American Statistical Association*, 105(491):1202–1214.
- Lunn, D., Best, N., Spiegelhalter, D., Graham, G., and Neuenschwander, B. (2009). Combining mcmc with ‘sequential’pkpd modelling. *Journal of Pharmacokinetics and Pharmacodynamics*, 36:19–38.
- Perera, C., Zhang, H., Zheng, Y., Hou, L., Qu, A., Zheng, C., Xie, K., and Liu, L. (2022). Hima2: high-dimensional mediation analysis and its application in epigenome-wide dna methylation data. *BMC Bioinformatics*, 23(1):296.

- Rimm, E. B., Giovannucci, E. L., Willett, W. C., Colditz, G. A., Ascherio, A., Rosner, B., and Stampfer, M. J. (1991). Prospective study of alcohol consumption and risk of coronary disease in men. *The Lancet*, 338(8765):464–468.
- Rubin, D. B. (1974). Estimating causal effects of treatments in randomized and nonrandomized studies. *Journal of Educational Psychology*, 66(5):688.
- Rubin, D. B. (1990). Formal mode of statistical inference for causal effects. *Journal of Statistical Planning and Inference*, 25(3):279–292.
- Saccenti, E., Hoefsloot, H. C., Smilde, A. K., Westerhuis, J. A., and Hendriks, M. M. (2014). Reflections on univariate and multivariate analysis of metabolomics data. *Metabolomics*, 10:361–374.
- Shan, Z., Wang, F., Li, Y., Baden, M. Y., Bhupathiraju, S. N., Wang, D. D., Sun, Q., Rexrode, K. M., Rimm, E. B., Qi, L., et al. (2023). Healthy eating patterns and risk of total and cause-specific mortality. *JAMA Internal Medicine*, 183(2):142–153.
- Song, Y., Zhou, X., Kang, J., Aung, M. T., Zhang, M., Zhao, W., Needham, B. L., Kardia, S. L., Liu, Y., Meeker, J. D., et al. (2021a). Bayesian hierarchical models for high-dimensional mediation analysis with coordinated selection of correlated mediators. *Statistics in Medicine*, 40(27):6038–6056.
- Song, Y., Zhou, X., Kang, J., Aung, M. T., Zhang, M., Zhao, W., Needham, B. L., Kardia, S. L., Liu, Y., Meeker, J. D., et al. (2021b). Bayesian sparse mediation analysis with targeted penalization of natural indirect effects. *Journal of the Royal Statistical Society Series C: Applied Statistics*, 70(5):1391–1412.

- Song, Y., Zhou, X., Zhang, M., Zhao, W., Liu, Y., Kardia, S. L., Roux, A. V. D., Needham, B. L., Smith, J. A., and Mukherjee, B. (2020). Bayesian shrinkage estimation of high dimensional causal mediation effects in omics studies. *Biometrics*, 76(3):700–710.
- Stingo, F., Chen, Y., Tadesse, M., and Vannucci, M. (2011). Incorporating biological information into linear models: a Bayesian approach to the selection of pathways and genes. *The Annals of Applied Statistics*, 5(3):1978–2002.
- VanderWeele, T. and Vansteelandt, S. (2014). Mediation analysis with multiple mediators. *Epidemiologic Methods*, 2(1):95–115.
- Wadsworth, W. D., Argiento, R., Guindani, M., Galloway-Pena, J., Shelburne, S. A., and Vannucci, M. (2017). An integrative Bayesian Dirichlet-multinomial regression model for the analysis of taxonomic abundances in microbiome data. *BMC Bioinformatics*, 18:1–12.
- Wang, D. D., Nguyen, L. H., Li, Y., Yan, Y., Ma, W., Rinott, E., Ivey, K. L., Shai, I., Willett, W. C., Hu, F. B., et al. (2021). The gut microbiome modulates the protective association between a mediterranean diet and cardiometabolic disease risk. *Nature Medicine*, 27(2):333–343.
- Wang, F., Baden, M. Y., Guasch-Ferré, M., Wittenbecher, C., Li, J., Li, Y., Wan, Y., Bhupathiraju, S. N., Tobias, D. K., Clish, C. B., et al. (2022). Plasma metabolite profiles related to plant-based diets and the risk of type 2 diabetes. *Diabetologia*, 65(7):1119–1132.
- Wang, F., Glenn, A. J., Tessier, A.-J., Mei, Z., Haslam, D. E., Guasch-Ferré, M., Tobias, D. K., Eliassen, A. H., Manson, J. E., Clish, C., et al. (2024). Integration of epidemio-

logical and blood biomarker analysis links haem iron intake to increased type 2 diabetes risk. *Nature Metabolism*, pages 1–12.

Wei, R., Wang, J., Su, M., Jia, E., Chen, S., Chen, T., and Ni, Y. (2018). Missing value imputation approach for mass spectrometry-based metabolomics data. *Scientific Reports*, 8(1):663.

Zhang, H., Zheng, Y., Zhang, Z., Gao, T., Joyce, B., Yoon, G., Zhang, W., Schwartz, J., Just, A., Colicino, E., et al. (2016). Estimating and testing high-dimensional mediation effects in epigenetic studies. *Bioinformatics*, 32(20):3150–3154.

Zhang, Q. (2022). High-dimensional mediation analysis with applications to causal gene identification. *Statistics in Biosciences*, 14(3):432–451.

Zhao, Y., Lindquist, M. A., and Caffo, B. S. (2020). Sparse principal component based high-dimensional mediation analysis. *Computational Statistics & Data Analysis*, 142:106835.

Zhao, Y. and Luo, X. (2022). Pathway lasso: Pathway estimation and selection with high-dimensional mediators. *Statistics and its Interface*, 15(1):39.

Zhao, Z., Banterle, M., Lewin, A., and Zucknick, M. (2024). Multivariate Bayesian structured variable selection for pharmacogenomic studies. *Journal of the Royal Statistical Society Series C: Applied Statistics*, 73(2):420–443.